25

POLYMER SOLUTIONS AND PROCESSING

Dámaso Navarro Rodríguez

25.1 INTRODUCTION

In simple terms, a polymer solution is a mixture of polymer and solvent molecules. The combination of these two chemical species, so different in size and properties, involves complex phenomena that have posed major challenges to engineers and scientists over the last 70 years. The difference in size is in fact the main origin of many dissimilar properties. A good illustration is the low viscosity of the majority of solvent liquids [1, 2] compared to the high viscosity of most polymer melts [3, 4]. In polymer solutions such a difference reflects in a large increase in viscosity with small increments in solute concentration [5]. The formation of a one-phase homogeneous polymer solution depends on the capacity of the solvent to dissolve the polymer [6]. In good solvents, polymers absorb, swell, disentangle, and finally disperse as individual molecules, except for crosslinked polymers or gels that absorb and swell as well, but to a limited degree without dissolution [7–11]. Thermodynamic parameters such as change in entropy (ΔS) and enthalpy (ΔH) of mixing play a crucial role in the formation of a polymer solution as well as in phase equilibria when phase separation occurs [12–14]. The entropy term describes the number of arrangements that the chains adopt in the system, whereas the enthalpy term accounts for the interactions between adjacent molecules [15]. Important factors are concentration, temperature, nature of both solvent and polymer, molecular weight of the polymer, among others [16–21].

Polymer solutions can be classified into five regimes (dilute, semidilute not entangled, semidilute entangled, concentrated not entangled, and concentrated entangled) [22] according to the polymer concentration and molar mass; however, it is much common to classify them into only three regimes of concentration (expressed in terms of polymer volume fraction, φ): dilute ($\varphi < \varphi^*$), semidilute ($\varphi \geq \varphi^*$), and concentrated ($\varphi^* \ll \varphi < 1$) solution [23]. The overlap concentration φ^* is not sharp, but it is rather a region at which polymer coils come close together and begin to overlap each other; experimentally, this could correspond to the condition where the concentration of the solution equals the average local concentration in the inside of the polymer coils [15, 24]. In a semidilute regime, the macromolecules are substantially overlapped, even though the solvent volume fraction is by far dominant. A more quantitative definition of these three concentration regimes can be found in various reports [25, 26]. Many studies on the physical and chemical properties of polymers have been conducted in dilute solutions, where the isolated polymer coils are relatively far apart from each other, and therefore the interchain perturbation may be negligible [27]. Under this low concentration regime, characteristics such as molecular weight, radius of gyration, number and frequency of long-chain branching, and some other structural parameters of the macromolecules can be readily determined [28–32]. Also, without difficulty, interactional parameters can be measured from dilute solutions [17, 33, 34]. On the other hand, semidilute and concentrated polymer solutions have also been very promising for the thermodynamic characterization of polymers [23, 35], although for these two regimes rheological studies have resulted particularly valuable to determine both structural and interactional characteristics [3, 5, 36]. It is to point out that, even though semidilute and concentrated polymer solutions are no longer appropriate to evaluate macromolecules individually, structure–property relationships in these regimes provide important information on these coiled molecules [23, 37].

Handbook of Polymer Synthesis, Characterization, and Processing, First Edition. Edited by Enrique Saldívar-Guerra and Eduardo Vivaldo-Lima.

At present, polymers are almost everywhere and, for many of their applications, particularly as fibers and films, they are processed from solution [38–41]. Dilute, semidilute, and concentrated polymer solutions are required for a wide variety of manufacturing processes, from the deposition of thin films over a substrate [spin coating, spraying, epitaxy, Langmuir–Blodgett (LB) deposition, etc.] to the processing of viscous polymer solutions or high polymer load dispersions (dip coating, wet and dry spinning, electrospinning, etc.) to obtain films and fibers with specific characteristics and properties.

In this chapter, a brief description on the fundamental aspects of polymer solution thermodynamics is given. Only some very basic or primary theories and their corresponding equations (simple approaches) are presented and discussed. For rigorous approaches and related advanced theories adequate references are given. As already mentioned, polymer solutions are required for a wide variety of processing techniques and even though most of such techniques were implemented on the basis of practical experience, much further work was done by engineers and scientists to refine them on the basis of polymer solution thermodynamics and rheology. There is abundant theoretical and empirical literature on the processing of polymers from solution; here, only some common processing techniques are briefly presented making special emphasis on spin coating, which at present time is extensively used for the deposition of thin films of a wide variety of polymers over a substrate.

25.2 POLYMER SOLUTION THERMODYNAMICS AND CONFORMATION OF POLYMER CHAINS: BASIC CONCEPTS

25.2.1 Change in Enthalpy, Entropy and Gibbs Free Energy of Mixing

In terms of thermodynamics, the solubility of a polymer in a solvent is determined from the free energy of mixing [42, 43]. In making a mixture, the internal energy (U) of a system changes from an initial to a final state. According to the first law of thermodynamics, a change in internal energy (ΔU) involves a flow heat from (or released to) the surroundings of the system and a work done on (or by) the system [44, 45]. At constant pressure P, the change in the enthalpy of mixing ΔH is

$$\Delta H = \Delta U + P\Delta V \tag{25.1}$$

where ΔV is the change in the volume of mixing.

On the other hand, the second law of thermodynamics stipulates that, in a spontaneous or nonreversible process, the entropy increases and the system moves toward a thermodynamically stable lower energy state, namely, state of equilibrium [46]. For binary systems the change in the entropy of mixing depends on the number of mixed molecules as follows:

$$\Delta S = k_B \ln \Omega_{1,2} \tag{25.2}$$

where k_B is the Boltzmann constant and $\Omega_{1,2}$ is the number of configurations or spatial arrangements that N_1 solvent molecules and N_2 solute molecules can adopt in the system (lattice) [47]. In contrast to a molecular solution (high ΔS value), in which both solvent and solute molecules are small, a polymer solution shows a much lower ΔS value because the number of configurations the joined mers (repeating units) can adopt in the lattice is much less important compared to that adopted by the same number of free mers [48]. In a spontaneous transformation, at constant pressure, the amount of heat a system (ΔH_{sys}) gives or receives is the same that the surroundings (ΔH_{surr}) receives or gives, respectively: $\Delta H_{sys} = -\Delta H_{surr}$. Thus, at constant temperature

$$\Delta S_{surr} = \frac{\Delta H_{surr}}{T} = -\frac{\Delta H_{sys}}{T} \tag{25.3}$$

According to the second law of thermodynamics, the entropy increases in spontaneous changes, $\Delta S_{sys} + \Delta S_{surr} > 0$, then

$$\Delta H_{sys} - T\Delta S_{sys} < 0 \tag{25.4}$$

The Gibbs free energy of mixing (ΔG) is the driving force for the composition of the mixture to change until the equilibrium is reached. The Gibbs free energy of mixing for a system is then defined as [44]

$$\Delta G_{sys} = \Delta H_{sys} - T\Delta S_{sys} \tag{25.5}$$

For a spontaneous process $\Delta G < 0$, for a nonspontaneous process $\Delta G > 0$, and for a system at equilibrium $\Delta G = 0$. Therefore, ΔG becomes an essential parameter that determines if a polymer will be spontaneously dissolved in a solvent or not.

At this point it is necessary to examine some basic concepts related to the polymer chain conformation that will certainly change in solution. In the solid state (amorphous or/and crystalline), the macromolecules contract and interpenetrate (entangle/co-crystallize) into the others, but once the solvent diffuses, they start to swell and eventually (high dilution) they disentangle to be finally dispersed in the solvent. In this process the polymer coils gradually expand reaching a conformational equilibrium dictated by thermodynamic laws. It was suggested that many properties of polymer solutions depend on the conformation of the chain, rather than on the nature of the chain atoms [45].

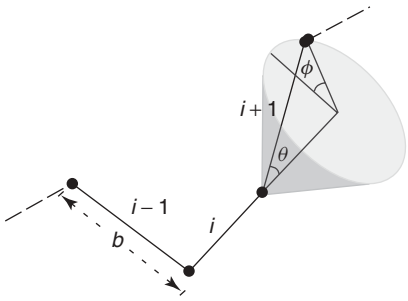

Figure 25.1 Basic geometrical parameters of a polymer chain.

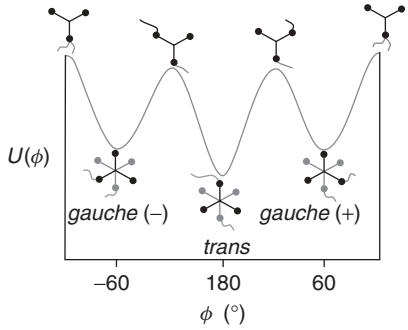

Figure 25.2 Energy diagram for the bond rotation.

25.2.2 Conformation of Polymer Chains

Statistical chain parameters can be readily determined from three geometrical parameters: the bond length (b), the angle (θ) between two successive bonds, and the bond rotation angle (ϕ) between the $i + 1$ and $i - 1$ bonds, projected on a disk generated by the 360° rotation of the i bond (Fig. 25.1) [48]. For a linear polymer chain, represented by a random coil, ϕ is normally restricted to just three values of minimal energy, 180, 60, and −60°, known as *trans*, *gauche*+, and *gauche*−, respectively (Fig. 25.2). There are also eclipsed positions at 0, 120, and −120°, which are energy barriers for the i bond to rotate. In surpassing one of these energy barriers (partial rotation) the relative position of the adjacent chain substituent groups changes, altering the local conformation. It is to point out that most thermal and mechanical properties of polymers are related to the extent of these energy barriers. If the energy barriers are not much larger than the thermal energy, the *trans*–*gauche* isomerization takes place easily, indicating that the chain is dynamically flexible [15].

One of the characteristic dimensions of polymer coils is the root-mean-square end-to-end distance ($\langle r^2 \rangle^{1/2}$), which for a linear chain of n bonds is calculated by considering the backbone bonds as vectors ($\boldsymbol{b}_i$) [49].

$$r_{ij}^2 = nb^2 + 2\sum_{i<j}^{n} \boldsymbol{b}_i \cdot \boldsymbol{b}_j \tag{25.6}$$

For a freely joined chain that consists of n' successive chain segments of fixed average length l' and bond angles between neighbor segments (uncorrelated), assuming all values with equal probability, the root-mean-square end-to-end distance is [50]

$$\langle r^2 \rangle_0 = n' l'^2 \tag{25.7}$$

The subscript zero indicates an unperturbed state and the angle brackets denote a statistical mechanical average. The length of a fully extended chain is nb or $n'l'$.

Another characteristic dimension is the radius of gyration ($\langle R_g^2 \rangle^{1/2}$), which is a root-mean-square distance calculated from the distances ($\boldsymbol{s}_i$) joining all segments of the chain to a center of gravity [48],

$$R_g^2 = \frac{1}{n}\sum_{i}^{n} s_i^2 \tag{25.8}$$

The radius of gyration is related to r_{ij} through the *Lagrange theorem*,

$$\langle R_g^2 \rangle = \frac{1}{2n^2}\sum_{i}^{n}\sum_{j}^{n} \langle r_{ij}^2 \rangle \tag{25.9}$$

$$\langle R_g^2 \rangle_0 = \frac{\langle r^2 \rangle_0}{6} \tag{25.10}$$

The parameters $\langle r^2 \rangle_0^{1/2}$ and $\langle R_g^2 \rangle_0^{1/2}$ correspond to an ideal chain. For the calculation of parameters of real chains, short- and long-range interactions may be considered. The former are related to local geometrical and interactional parameters such as fixed bond angles and potentials perturbing bond rotations, whereas the latter are mainly related to interactions involving remote units in the chain. As is discussed later, the long-range interactions can be eliminated through experimental procedures; the unperturbed dimensions thus obtained may be interpreted only in terms of short-range features [49].

The dimensions $\langle r^2 \rangle^{1/2}$ and $\langle R_g^2 \rangle^{1/2}$ are single-average distances of a very large number of possible conformations. By means of probability tools, the distribution function $W(r)$ of all possible r^2 can be deduced [45, 49]. For ideal polymer chains this function is Gaussian,

$$W(r) = \left(\frac{3}{2\pi \langle r^2 \rangle}\right)^{3/2} e^{-3r^2/2\langle r^2 \rangle} \tag{25.11}$$

It should be said that a Gaussian coil is not appropriate for the representation of real polymer chains because it does not take into account volume effects produced by long-range interactions. A polymer chain in a random walk cannot cross its own path. In other words, a real

polymer chain has excluded volume, which disallows a number of chain conformations. As a consequence, the polymer coil swells reaching a larger dimension than that normally calculated for a Gaussian coil. Exact numerical and analytical self-avoiding walk models were developed for a more accurate calculation of the chain parameters [51–53]. It was demonstrated that the radius of gyration of real chains scales as N^{ν} (ν is approximately 3/5) and not as $N^{0.5}$, as deduced for ideal chains. Experimental and theoretical approaches were proposed to determine the value of ν [54, 55]. One approach is the exact enumeration of self-avoiding walk models, which considers a limited number of computed walks, but is accurate when precise and refined extrapolation methods are used [56]. Another approach is through Monte Carlo methods in which quite long walks can be sampled, but the data are necessarily subjected to statistical uncertainty [55]. By considering excluded volume effects, an acceptable value of 0.588 (for $d = 3$ dimensions) was estimated by Monte Carlo methods.

25.2.3 Flory–Huggins Lattice Theory and Related Theories

When a number of polymer molecules (N_2) are mixed with a number of molecules of a good solvent (N_1) they disperse and at the same time they expand from a constricted dimension. Hereafter, in this section the subscripts 1 and 2 refer to the solvent and the polymer in the mixture, respectively. The resulting polymer solution can be examined from the Flory–Huggins theory, in which a 3D lattice of sites is filled with solvent and polymer molecules; each site of the lattice being occupied either by a solvent molecule or by a polymer segment whose size or volume is similar to that of the solvent molecule [42, 43]. Under this consideration, the volume of a polymer chain (V_2) is r times the volume of a solvent molecule (V_1). The volume fraction of the polymer (φ_2) in the lattice is then $N_2\ r/(N_1 + N_2 r)$. Compared to a solution in which both solvent and solute molecules are small, the combinatorial calculated number of configurations for a polymer solution may be much smaller due to the fact that the contiguous segments of a polymer chain are constrained to occupy only adjacent sites. The logarithm of the number of calculated configurations for a polymer solution in terms of volume fraction is $\ln \Omega_{1,2} = -(N_1 \ln \varphi_1 + N_2 \ln \varphi_2)$ [45]. For an ideal or athermal solution ($\Delta H = 0$), the intermolecular interaction energy between mixed species is the same ($\varepsilon_{11} = \varepsilon_{22} = \varepsilon_{12}$), then

$$\Delta G = -T\Delta S = k_B T \left(N_1 \ln \varphi_1 + N_2 \ln \varphi_2\right) \tag{25.12}$$

In this relation, ΔG is always negative, because the mole fractions are always less than unity.

Polymer solutions are in general considered as regular solutions for which the intermolecular interaction energy between the mixed species is different from one another ($\varepsilon_{11} \neq \varepsilon_{22} \neq \varepsilon_{12}$) and then $\Delta H \neq 0$ [47]. In these solutions the change in the entropy of mixing is considered similar to that calculated for ideal solutions. This simplification may be acceptable for polymer solutions of low polar character. The change in the enthalpy of mixing for regular solutions is

$$\Delta H = N_1 \varphi_2 z\, \Delta\varepsilon \tag{25.13}$$

where z is the lattice coordination number and $\Delta\varepsilon$ is the energy of mixing for each contact. So, the change in the Gibbs free energy of mixing for a regular solution is [48]

$$\Delta G = k_B T \left(N_1 \ln \varphi_1 + N_2 \ln \varphi_2 + N_1 \varphi_2 \chi_{1,2}\right) \tag{25.14}$$

where $\chi_{1,2}$ is a dimensionless parameter known as the *Flory interaction parameter.*

From this equation, the chemical potential of mixing per moles of component $i(\Delta\mu_i)$ can be calculated [48]. For a binary mixture,

$$\Delta\mu_1 = \left(\frac{\partial \Delta G}{\partial N_1}\right)_{T,P,N_2} \tag{25.15}$$

$$\Delta\mu_1 = k_B T \left[\ln \varphi_1 + \left(1 - \frac{1}{r}\right)\varphi_2 + \chi_{1,2}\varphi_2^2\right] \tag{25.16}$$

In this equation, $\chi_{1,2}$ is independent of composition and enthalpic nature; however, experiments have demonstrated that this is not necessarily true [16, 20, 57].

For a dilute solution $\ln(1 - \varphi_2) \approx -\varphi_2 - \varphi_2^2/2$, and taking into account that $V_2/V_1 = r$ and $\varphi_2 = CV_2/M_2$

$$\Delta\mu_1 = -RT \left[\frac{CV_1}{M_2} + \left(\frac{1}{2} - \chi_{1,2}\right)\left(\frac{CV_2}{M_2}\right)^2\right] \tag{25.17}$$

where C is the concentration of the solution, R is the gas constant, M_2 is the molecular weight of the polymer, and V_1 and V_2 are the partial molar volumes of the solvent and polymer, respectively.

It is to note that this simple equation was deduced assuming a random mixing process, a volume change upon mixing that vanishes, and an interaction parameter $\chi_{1,2}$ independent of composition, among others [58, 59]. In spite of these simplification criteria, and others of subtle nature, the equation gives a qualitative insight into the nature of polymer solutions.

The change in the chemical potential of the solvent is related to the osmotic pressure (π) through a simple expression $\Delta\mu_1 = -\pi\ V_1$ [17], then

$$\pi = RT \left[\frac{C}{M_2} + \left(\frac{1}{2} - \chi_{1,2}\right)\left(\frac{V_2}{M_2}\right)^2 \left(\frac{1}{V_1}\right) C^2\right] \tag{25.18}$$

This second-degree polynomial equation can be simply represented as

$$\frac{\pi}{RTC} = \frac{1}{M_2} + A_2 C \tag{25.19}$$

where A_2 is the osmotic second virial coefficient. A_2 and M_2 can then be deduced by measuring the osmotic pressure of a series of diluted polymer solutions. The value of A_2 can be either positive or negative depending on the experimental temperature [17]. The temperature at which $A_2 = 0$ is known as the Flory temperature or *theta* temperature. $A_2 = 0$ for $\chi_{1,2} = 0.5$, which is a critical value of miscibility of a polymer in a solvent [16]. In most cases, $\chi_{1,2}$ is positive because interactions are mainly van der Waals attractions [15]. For good solvents $\chi_{1,2}$ is much smaller than 0.5. For $\chi_{1,2} = 0.5$ it is supposed that the attractive and repulsive forces between the polymer and the solvent are completely compensated and the polymer chains are considered to be under unperturbed conditions (ideal chains) [35].

Light scattering measurements can also be used to determine the molecular weight (M_2) of solute molecules as well as interactional (second and third virial coefficients) and structural parameters (radius of gyration) [60, 61]. The reader is referred to Chapter 18 for more information on light scattering methods. The dependence of A_2 and $\langle R_g^2 \rangle$ on M have been the subject of many research studies in polymer solution thermodynamics [29, 62]. Many other experimental techniques can been used to determine these and other related parameters [28, 35, 63].

The Flory–Huggins lattice theory has been considered the basis of the polymer solution thermodynamics and many of further theories on this subject have been either simple or complex modifications, aiming to overcome deficiencies that have arisen from simplifications used in the original equation. Flory and Krigbaum developed the Flory–Huggins theory by taking into account alternate regions of pure solvent and solvated polymer domains, and introduced the concepts of excluded volume and *theta* temperature [27]. Heil and Prausnitz [16] have derived a semiempirical equation containing two adjustable parameters, which is a compromise between the relatively simple one-adjustable parameter equation of Flory–Huggins and the complex multiparameter theories of later authors. Their so-called segment-interaction equation, which makes use of the local volume fraction concept, first stipulated by Wilson [64], was successfully applied to a variety of polymer solutions including polymer-mixed solvent systems having specific interactions such as hydrogen bonding. Renuncio and Prausnitz have proposed an approximation introducing nonrandomness to the Flory–Huggins equation [65]. For that purpose they have also used the Wilson local composition concept. The residual entropy calculated under this assumption was different from that of the Flory–Huggins equation. The calculated change in the enthalpy of mixing and activity data that they applied to a few binary polymer–solvent systems was consistent with experimental results. Alternative expressions of this model were later proposed making the theory more realistic [66]. Sanchez–Lacombe developed a molecular theory on pure fluids of variable geometry and size that was later generalized to mixtures [67, 68]. Their model, which considers occupied and vacant lattice sites (holes), makes a complete thermodynamic description of the fluid that is useful to predict liquid–vapor transitions and the effect of chain length on the critical and boiling point of normal alkanes, among others. A similar model, which introduces a nonrandom distribution of mixing to pure-hole components and polymer solutions, was later proposed [69]. Examples of other approaches and refinements of the Flory–Huggins theory can be found in the literature, all of them aiming at improving predictions on the polymer solution properties [21, 70–72].

25.2.4 The Solubility Parameter

The choice of an appropriate solvent to dissolve a polymer is frequently based on experience or guided by literature and technical reports on some solvent characteristics such as solvent "strength," rate of evaporation, and solvent/nonsolvent mixture effects, among others; some of these characteristics may have strong effects on both the polymer processing from solution and the properties of the final product. Theories on polymer–solvent mixtures are of essential importance and could be developed to understand the thermodynamics of the system but, sometimes, they can be extremely complex to be developed and applied in ordinary polymer solutions that are going to be processed. Alternatively, numerous simple and practical methods reported in the literature can be used for the prediction of the solubility behavior in polymer solutions [13, 19]. One of the most practical methods uses the Hildebrand solubility parameter (δ), which is a numerical value related to the intermolecular interactions (van der Waals) that hold together the molecules in a solvent or in a solid. For a small amount of a solid (solute) in a solution those interactions are disrupted by the solvent in such a way that the individual solute molecules separate from one another. Such a disruption seems to be optimal when the solute–solute and solvent–solvent molecular interactions are of similar "strength." Thus, solvents and solids (polymers) showing similar δ values may dissolve in the other and form miscible mixtures; through this simple rule the solubility of a polymer in a solvent can be practically predicted [70].

The solubility parameter is defined as the square root of the cohesive energy density per unit volume and for a solvent it can be obtained from the heat of vaporization $\left(\Delta E_i^{\text{vap}}\right)$, which is the energy supplied to vaporize a fluid [70]. This property is particularly helpful because it is

supposed that the same intermolecular forces should be overcome to vaporize a liquid and to dissolve it.

$$\delta_i = \left(\frac{\Delta E_i^{\text{vap}}}{V_i} \right)^{1/2} \tag{25.20}$$

There is no way to determine the solubility parameter of polymers by means of the heat of vaporization; instead, swelling experiments, methods involving cloud-point determinations, and some others are used to determine it [13].

The Flory interaction parameter is related to the solubility parameter through the following equation:

$$\chi_{1,2} = \frac{V_1}{RT} \left(\delta_1 - \delta_2 \right)^2 \tag{25.21}$$

where δ_1 and δ_2 are the solubility parameters of the solvent and the polymer, respectively, and V_1 is the partial molar volume of the pure solvent.

This equation takes into account only enthalpic contributions; however, for a best calculation of the Flory parameter $\chi_{1,2}$, the entropic contributions, χ_s, should be considered as well [70, 73].

$$\chi_{1,2} = \chi_s + \frac{V_1}{RT} \left(\delta_1 - \delta_2 \right)^2 \tag{25.22}$$

In terms of solubility parameters, the change in the enthalpy of mixing is

$$\Delta H = n_1 V_1 \varphi_2 \left(\delta_1 - \delta_2 \right)^2 \tag{25.23}$$

This equation clearly shows that ΔH tends to zero when δ_1 and δ_2 approach each other. In this case, $\Delta G < 0$ is expected, and good solubility properties will be observed with small mixing heats. It has been reported that miscibility should occur for values of δ_1 and δ_2 within 2 or 3 $J^{1/2}$ $cm^{-3/2}$ of one another [74].

An extension of the Hildebrand parameter to estimate the relative miscibility of polar and hydrogen bonding systems has been proposed: $\delta^2 = \delta_d^2 + \delta_p^2 + \delta_h^2$. The components of this equation are the dispersion $\left(\delta_d^2\right)$, electrostatic (or polar) $\left(\delta_p^2\right)$, and hydrogen bond $\left(\delta_h^2\right)$ Hansen solubility parameters [75, 76].

Numerous sources with compiled solubility parameters are available for commercial solvents [1, 2] and polymers [2, 73] Although their use affords qualitative results, they are commonly used in industry to predict the miscibility of polymers in solvents [39, 77]. For solvents ranked according to their solubility parameter, those in close proximity may show a comparable solubility behavior, whereas those that are far apart may show substantial differences.

25.2.5 Phase Equilibria in Polymer Solutions

Phase separation is frequently observed in polymer solutions and it is mainly due to their low entropy of mixing. At a state of equilibrium each species of the mixture is partitioned between two phases, namely, the supernatant (extremely dilute) and precipitated (moderately dilute) phases [78]. Theoretical models and experimental techniques have been developed to predict the solubility behavior of polymer solutions, polymer blends, and other related systems [79, 80]. Simple theories only permit a rather qualitative description of this phenomenon [78]. Refined and improved theoretical and semiempirical models allow a more accurate prediction of the demixing phenomena and related thermodynamic properties [57, 81].

At a given pressure and temperature, the total Gibbs free energy of mixing of a one-phase polymer–solvent system of composition φ_2 should be necessarily minimum, otherwise the system will separate into two phases of different composition, as it is represented in a typical ΔG versus φ phase diagram of a binary solution (Fig. 25.3). The volume fractions at the minima ($\partial \Delta G / \partial \varphi = 0$), φ', and φ'', will vary with temperature (*binodal*) up to critical conditions (T_c and φ_c) where $\varphi' = \varphi''$ (Fig. 25.3b).

According to the type of T versus φ diagram (Fig. 25.4), the binary solution can exhibit an upper critical solution temperature (UCST), a lower critical solution temperature (LCST), or both (close-loop phase behavior). Above the UCST or below the LCST the system is completely miscible in all proportions [82]. Below the UCST and above LCST a two-phase liquid can be observed between φ' and φ''. The two-phase liquid can be subdivided into unstable (spontaneous phase separation) and metastable (phase separation takes some time). These two kinds of mixtures are separated by a *spinodal*, which is outlined by joining the inflexion points ($\partial^2 \Delta G / \partial \varphi^2$) of successive ΔG versus φ phase diagrams, obtained at different temperatures (Fig. 25.3b). Thus, the binodal and spinodal touch each other at the critical points φ_c and T_c.

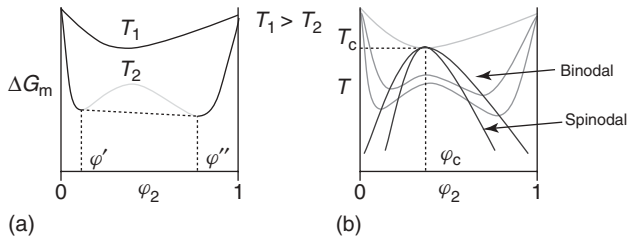

Figure 25.3 Binary phase diagrams. (a) At T_1 the mixture is miscible at all composition and at T_2 the mixture shows phase separation (between φ' and φ''). (b) Binodal and spinodal curves, and critical temperature (T_c) and concentration (φ_c).

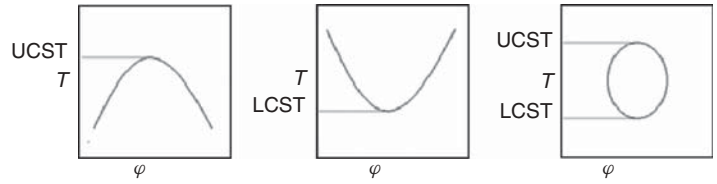

Figure 25.4 Temperature–volume fraction diagrams for binary polymer solutions.

From Equation 25.16 the conditions for incipient phase separation are [12, 45]

$$\left(\frac{\partial \mu_1}{\partial \varphi_2}\right)_{T,P} = 0 \quad \text{and} \quad \left(\frac{\partial^2 \mu_1}{\partial \varphi_2^2}\right)_{T,P} = 0 \tag{25.24}$$

The combination of the resulting expressions gives [48]

$$\varphi_c = \frac{1}{1+\sqrt{r}} \tag{25.25}$$

and

$$\chi_c = \frac{1}{2}\left(1+\frac{1}{\sqrt{r}}\right)^2 \cong \frac{1}{2}+\frac{1}{\sqrt{r}} \tag{25.26}$$

Then, the critical concentration (φ_c) depends on the relative size (molecular weight) of the components of the mixture. For mixtures involving small molecules $\left(\sqrt{r}=1\right)$, φ_c takes a value of around 0.5; however, for polymer solutions the phase diagram (Fig. 25.5) becomes highly asymmetric with φ_c essentially confined to the solvent-rich regime ($\varphi_c \to 0$ for $r \to \infty$).

Flory has proposed that

$$\frac{1}{2} - \chi_{1,2} = \psi\left(1-\frac{\theta}{T}\right) \tag{25.27}$$

where ψ is the entropy of dilution parameter.

At the temperature where phase separation occurs $T = T_c$, then

$$\frac{1}{T_c} = \frac{1}{\theta}\left(1+\frac{1}{\psi\sqrt{r}}\right) \tag{25.28}$$

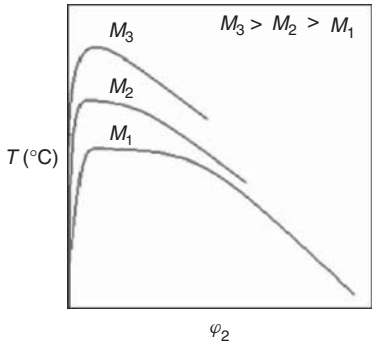

Figure 25.5 Phase diagrams for polymer/solvent mixtures.

This equation shows that the critical temperature (T_c) is also dependent on the molecular weight of the polymer [82]. Thus, for a UCST diagram this critical parameter moves toward higher temperatures as the chain length increases (Fig. 25.5). This dependence is particularly useful for the fractionation of most synthetic polymers, which are seldom molecularly uniform [83].

At equilibrium, the two-phase coexistence is conditioned to an identical chemical potential of components (i) between phases $\left(\Delta\mu_i' = \Delta\mu_i''\right)$. The chemical potential is a valuable parameter because it is directly related to experimentally accessible properties, as is the case of the osmotic pressure, $\pi = -\Delta\mu_1/V_1$.

Initial works on the phase equilibrium of polymer solutions were concerned with nonpolar solutions using carefully prepared quasi-monodisperse polymer fractions [78]. The theory and practice was later extended to molecularly heterogeneous polymers [84], multicomponent solutions (ternary mixtures) such as polymer/solvent mixture [16, 85] and polymer mixture/solvent [86], and polymer blends [79, 80], among others [87]. Improvements on predicting thermodynamic properties were particularly proposed for polymer solutions of industrial importance, including those having polar and hydrogen-bonded components [16].

25.2.6 Characterization of Polymers Using Thermodynamic-Based Techniques

Characterization of polymers in solution has posed unique challenges owing to their inherent complexity, primarily associated to their high molecular weight, chemical structure, and composition. Such complexity is accentuated by the fact that most polymers exhibit a molecular weight distribution and structural defects. For the characterization of polymers in solution there exist well-developed instrumentation and methodologies. The most common techniques are as follows:

- NMR, FTIR, UV–vis—chemical and structural characterization (see Chapter 16)
- GPC (or SEC), MALDI-TOF—molecular weight and MWD (see Chapters 17 and 16, respectively)
- LS, Neutron scattering—molecular weight, structural and interactional parameters (see Chapter 18)
- Viscometry—molecular weight, flow properties, and structural and interactional parameters

MO, VPO, Eb., Cry.[1] —molecular weight and interactional parameters.

All these techniques use different principles of measurement. Here, only two methods based on colligative properties are described.

The number-average molecular weight (M_n) of polymers can be easily determined from methods based on colligative properties, which are dependent on the number of molecules in the solution [28]. Thus, the addition of a number of solute molecules to a solvent produces a change in the chemical potential ($\Delta\mu_1$) of the solvent from which the molecular and interactional parameters can be deduced.

Among the different techniques based on colligative properties, the most practical ones to determine M_n (number-average molecular weight) are the MO [17, 28] and the VPO [88], both performed in dilute solution.

25.2.6.1 Membrane Osmometry In this technique a dilute polymer solution and a pure solvent are separately placed in two different chambers that are divided by a tightly held semipermeable membrane through which only solvent molecules can move across. Because the chemical potential of pure solvent is higher than that of the solvent in the solution, the solvent will diffuse across the membrane from the pure solvent to the solution chamber up to the point in which the osmotic pressure equals the hydrostatic pressure created by the volume imbalance between the liquids of the two chambers. The osmotic pressure ($\pi = \rho g h$) at equilibrium (static method) can be calculated from the difference in height (h) between the liquids in the capillaries connected to each chamber. In practice, a dynamic method is used in which a pressure (P) is applied to counterbalance (at $t = 0$) the osmotic pressure (π) exerted by the pure solvent. This later method is known as *dynamic osmometry* and allows an instantaneous determination of π [17, 89].

For a series of dilute solutions (C_1, C_2, C_3, $C_4 \ldots$) at constant temperature [60],

$$\frac{\pi}{C} = RT\left(\frac{1}{M_n} + A_2C + A_3C^2 + \cdots\right) \qquad (25.29)$$

The first term of this equation is the van't Hoff expression ($\pi/C_{c\to 0} = RT/M_n$) for osmotic pressure at infinite dilution and the second term is related to the second virial coefficient (A_2). Thus, M_n and A_2 can be, respectively, determined from the intercept and the slope from a π/C versus C plot (the third and higher virial coefficient terms are normally ignored) [90]. Compared to other experimental techniques (SEC and light scattering), MO is limited to the study of a relatively narrow molar mass range $10^3 - 5 \times 10^5$ g/mol, which depends on the membrane permeability (low molar mass limit) and on the smallest osmotic pressure that can be reliably measured (upper molar mass limit). As mentioned above, A_2 is a measure of polymer–solvent interactions and its value is an indication of the capacity of the solvent to dissolve a polymer at determined conditions. Good solvents show positive values typically in the order of $10^{-4} - 10^{-3}$ (ml mol)/g^2. At *theta* conditions $A_2 = 0$, where polymer molecules are supposed to be under unperturbed conditions. It is common to build $(\pi/C)^{0.5}$ versus C plots because they are normally linear over broader ranges of concentration compared to those of π/C versus C plots. The main advantage of this technique is that calibration with standards is not required, yielding an absolute number-average molecular weight (M_n).

25.2.6.2 Vapor Pressure Osmometry The VPO became a popular method for the determination of the number-average molecular weight of nonvolatile solutes of less than about 20,000 g/mol and that tend to diffuse across the membrane in MO experiments [91]. This method operates on the principle that the vapor pressure of a solution is lower than that of a pure solvent $\left(P_1^0\right)$ at constant pressure and temperature. This vapor pressure lowering (ΔP) is proportional to the molar mass of the solute (polymer) for dilute solutions. As it is known, the vapor pressure of a solvent in dilute solutions obeys the Raoult's law, $P_1 = P_1^0 x_1$, where P_1 is the partial vapor pressure of the solvent whose mole fraction in the solution is x_1. In terms of the mole fraction of the solute, $P_1 = P_1^0\left(1 - x_2\right)$ or $\Delta P/P_1^0 = -x_2$.

As measuring vapor pressure depression using VPO requires extreme sensitivity, a thermoelectric method is used based on the following principle. One drop of pure solvent is placed on one of two matched temperature-sensitive thermistors located in a chamber saturated with vapor solvent, at constant temperature. On the other thermistor, a drop of polymer solution is placed. The solvent condensation on the solution drop will heat it up until its vapor pressure matches that of the pure solvent drop [35].

From thermodynamics,

$$\Delta T = \frac{RT^2 x_2}{\Delta H_{vap}} \qquad (25.30)$$

For dilute solutions $x_2 \approx n_2/n_1$, and, if the polymer concentration (C_w) is expressed in grams of solute per 1000 g of solvent (molality),

$$\Delta T = \frac{RT^2}{\Delta H_{vap}} \times \frac{C_w}{M_n} \times \frac{m_1}{1000} \qquad (25.31)$$

where m_1 is the molar mass of the solvent.

[1]MO, membrane osmometry; VPO, vapor pressure osmometry; Eb., ebullometry; Cry., cryoscopy.

The temperature change causes a resistance change (ΔR) in the thermistor and for practical reasons ΔR measurements are preferred instead of direct measurements of ΔT. ΔR is directly proportional to ΔT for small changes in temperature ($\Delta R \propto \Delta T$) [92]. In this method substances of known molecular weight are used to determine the calibration constant of the instrument. A calibration curve relates the change in resistance to the molal concentration of the solution. The molecular weight of the polymer can then be determined from the resistance measurements through the following equation [91]:

$$\left(\frac{\Delta R}{C}\right)_{C\to 0} = \frac{K}{M_n} \tag{25.32}$$

Details on the methodologies and instruments for MO and VPO can be found elsewhere [17, 28, 90].

25.3 SEMIDILUTE POLYMER SOLUTIONS

The thermodynamic behavior of semidilute polymer solutions is substantially different from that of dilute solutions [15]. In the semidilute regime ($\varphi > \varphi^*$), the chains interpenetrate each other reducing their overall motion. Under this condition, viscosity and the osmotic pressure of the solution rapidly increase with small changes in concentration [26, 93]. The overlap concentration (φ^*) decreases as the chain length (or N) increases and, consequently, the range of the semidilute regime widens, although the upper limit is ambiguous to define.

The mean field theory seems to be helpful in explaining the behavior of semidilute solutions, but it fails in explaining various experimental results [35]. Alternative theories such as the blob concept and the scaling theory, both introduced in the 1970s, have been successfully applied to determine the thermodynamic behavior of these solutions [15].

25.3.1 The Blob Model

Between two neighboring entanglement points of the same chain there is a segment that occupies a domain or sphere (blob) and that adopts its conformation independently of other segments (Fig. 25.6). The chain segment within the blob takes a similar conformation to that of the whole chain. As this concept applies to all chain segments, the entire solution is implicitly composed of blobs.

At the overlap concentration φ^*, in a good solvent ($v = 3/5$), the overall monomer density (ρ^*) is [15, 26]

$$\rho^* \cong N \ R_g^{-3} \cong b^{-3}N^{-4/5} \tag{25.33}$$

A blob of size ξ has g monomers of size b, then $\xi \cong bg^v$. Also, the density of monomers within the blob is $\rho \cong g\xi^{-3}$.

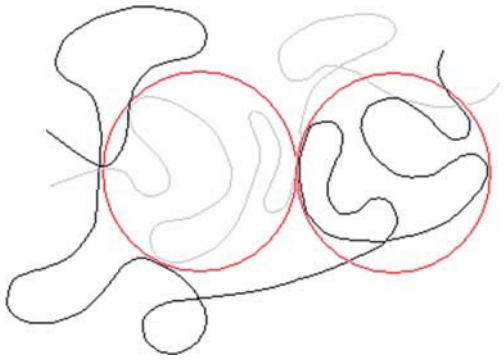

Figure 25.6 Representation of blobs in a polymer chain. (*See insert for the color representation of the figure*.)

The combination of these two relations ($\xi \cong b^{-5/4}\rho^{-3/4}$) indicates that the blob size decreases with concentration. It can also be noticed that ξ is determined only by the monomer density and not by N.

The blob size relative to the mean-square radius of gyration is

$$\xi \cong R_g \left(\frac{\rho}{\rho^*}\right)^{-3/4} \tag{25.34}$$

and the number of monomers in the blob is

$$g \cong N \left(\frac{\rho}{\rho^*}\right)^{-5/4} \tag{25.35}$$

For $\rho = \rho^*$, $\xi = R_g$ and $g = N$. At $\rho > \rho^*$ both ξ and g decrease (Fig. 25.7) because the chains become more densely overlapped with each other.

In ideal solutions, the polymer chain moves as a unit. The osmotic pressure for this solution is

$$\pi_{C\to 0} = \frac{\rho}{N} k_B T \tag{25.36}$$

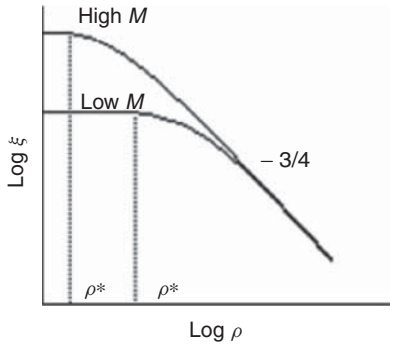

Figure 25.7 Blob size as a function of monomer density for two different chain lengths.

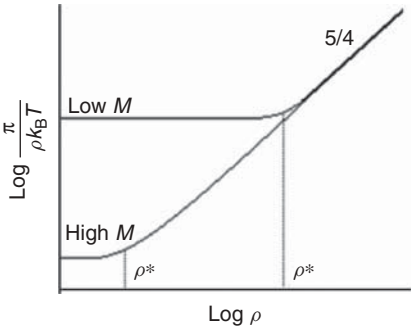

Figure 25.8 Osmotic pressure reduced by $\rho\ k_B T$ as a function of monomer density for two different chain lengths.

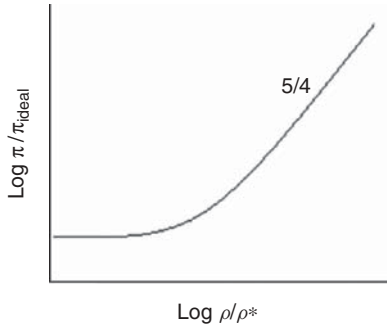

Figure 25.9 Reduced osmotic pressure as a function of reduced concentration.

For semidilute solutions the segment of a blob moves as a unit. The osmotic pressure for this solution depends on the number of blobs per unit volume ($1/\xi^3$).

$$\pi \cong k_B T \xi^{-3} \cong k_B T \ \ b^{-15/4} \rho^{-9/4} \tag{25.37}$$

This relation indicates that in a semidilute regime π is the same for solutions of polymers of different chain length or molecular weight (Fig. 25.8); thus, at $\rho > \rho^*$ the osmotic pressure is independent of M, contrasting with the behavior of a dilute solution, in which π is strongly dependent on M.

25.3.2 Scaling Theory

In the scaling theory, introduced by de Gennes [15], the osmotic pressure behaves like some powers (m) of concentration and becomes independent of the degree of polymerization (N). For semidilute solutions (large x),

$$\frac{\pi}{k_B T} = \frac{\rho}{N} f_{II}(x) = \frac{\rho}{N} \text{const} \left(\frac{\rho R_g^3}{N} \right)^m \tag{25.38}$$

where f_{II} is the scaling function. As $R_g = bN^{3/5}$,

$$\frac{\pi}{k_B T} = \text{const} \ \ b^{3m} \rho^{m+1} N^{(4m/5)-1} \tag{25.39}$$

For $m = 5/4$, π is independent of N and dependent on $\rho^{9/4}$ [17, 26]. The dependence of π on ρin the mean field theory (ρ^2) is different from that in the scaling theory ($\rho^{9/4}$) by a factor of $\rho^{1/4}$. Such difference is related to a correlation effect given by the number of contacts between monomers. The reduced osmotic pressure (π/π_{ideal}) plotted as a function of the reduced concentration (ρ/ρ^*), in a double logarithm scale, displays a curve that shows the change in slope to 5/4 for $\rho/\rho^* > 1$ (Fig. 25.9).

25.4 PROCESSING OF POLYMER SOLUTIONS

A large number of solution-based processing methods have been used for manufacturing films and fibers from a wide variety of commercial polymers [94–96]. These methods are in fact ideal for the processing of nonmelting but soluble polymers or for the processing of thermally sensitive polymers. Also, they are often the most appropriate methods for the fabrication of very thin films and fibers that cannot be produced by melt extrusion, and they are particularly useful to deposit functional thin and ultrathin films over a wide variety of substrates.

25.4.1 Film Forming Processes via Polymer Solution

25.4.1.1 Solvent Casting Solvent casting is a method for manufacturing films from a solution or dispersion [96]. In a standard process, the polymer and other components are dissolved in a solvent and the resulting solution is poured into a mold (usually an open vessel) where the solvent evaporates leaving a residual film [97, 98]. Two main technologies, the wheel and the belt (or band) casting processes are used in the industry to cast continuous polymer films from solution (Fig. 25.10; 94, 99). The essential elements of these processes are the dope preparation, the film deposition, and the film drying. The dope is a polymer solution or dispersion normally prepared using low vapor pressure solvents; it may contain some other components like plasticizers, ultraviolet absorbers, antistatic compounds, and release agents [100]. Standard mixers are used to disperse the polymer and other solids (or liquids) in the solvent or mixture of solvents to form a homogenous dispersion that should be stable before and during the film forming process [101]. The rheological properties of the solution depend, among others, on the concentration of solids, which typically ranges between 5% and 40%, and on the temperature, which can vary between room temperature and the boiling point of the solvents [96, 102]. The dope is normally degassed to prevent the

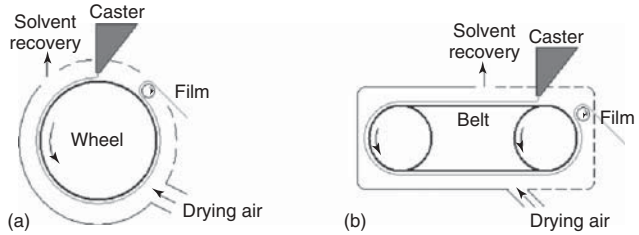

Figure 25.10 Schematic representation of the (a) wheel and (b) belt casting processes.

formation of air bubbles during the film forming process [103]. A filtration or clarification system is required to eliminate gels, agglomerates, or some other undesirable particles. The dope is continuously deposited as a thin film of uniform thickness over an endless moving surface (wheel or belt) that requires an accurate speed control. The surface finish of the casting support is critical, taking into account that the surface is accurately replicated onto the contact surface of the casted film. Specially designed casters or dies are used to homogeneously distribute the dope across the moving surface. For best results, the flow rate in the die may not exceed that corresponding to laminar flow. The film drying can be performed through different methods, including airstream and radiation heating, at relatively soft conditions. The solvent evaporates all along the film forming process while it is evacuated and conducted up to a solvent recovery system. The evaporation rate of the solvent depends on the solids' content, which continuously increases as the solvent evaporates [104]. Solvent evaporation takes place in essentially two stages: in the first stage it is governed by the vapor pressure, but as long as the polymer solidifies the solvent is retained within the film and it is lost in the second stage by a diffusion-controlled process [105]. Before the takeoff point, the film is cooled down to reduce tackiness and to increase its mechanical strength. Once detached from the support, the semifinished film is air dried at both open surfaces in further steps to be finally winded.

25.4.1.2 Coating Coating is a process of deposition of a thin film over a surface or substrate to change its characteristics and properties [39, 106]. Also, the term coating describes any material applied as a thin continuous layer to a surface. A wide variety of coating processes can be performed from solution, the choice of one of them depends on the characteristics and/or properties of the solution, the substrate, the polymer and other components, the solvent, and the final film, among others [107]. More recent influences on the choice of the coating process are environmental considerations, health and safety legislations, and cost/benefit relationships [39]. Of primary importance are solvents, which play a crucial role as diluents of the polymer and other nonvolatile components [108]. Most diluents are organic solvents, although for specific applications or for environmental reasons diluents such as water are preferred [109, 110]. The flow properties are highly dependent on the polymer/solvent characteristics and their relative amounts in the solution [111]. Once the solution is deposited, the solvent evaporates leaving a regular film adhered to the substrate, which is composed solely of the nonvolatile components. In general, deposited films are soluble if they were solidified by evaporation of the solvent, but they become insoluble if they are cured (crosslinked) through chemical reactions [112, 113]. The film thickness depends on the solution concentration (density), viscosity, polymer characteristics, and deposition speed, among others [114–117]. Multilayer films can be deposited from the same or different coating solution by means of successive coatings [118, 119].

The most important coating processes for the deposition of polymer films from solution are spreading, spraying and flow coating. Spreading (e.g., brush and roller) and spraying (e.g., air spray) are the most extensively used methods for the application of architectural and industrial coatings or paints [39]. Flow coating processes are automated methods for the application of industrial liquids (coatings) over a moving surface. They may be broadly classified into two categories: self-metered and premetered [120]. Self-metered ones include dip as well as roll and blade coating, while premetered ones comprise slot, slide, and curtain coating [121]. In self-metered coating methods a reservoir is normally used for direct or indirect coating. A blade often serves as a metering flow element. In premetered coating methods, a coating die delivers and distributes the desired amount of one or more coating flows. The following are simple schematic configurations of various common coating processes used for the deposition of polymer films (Fig. 25.11).

Following are the important steps in coating processes: preparation of the coating solution, deposition of the solution over a substrate, and finally the solidification of the deposited film (drying or curing). Most industrial coating processes use automated coaters, although for some specific coating needs hand application methods are still preferred.

In relatively recent years, singular coating processes have emerged to comply with specific application needs, especially for the deposition of functional or advanced thin and ultrathin films. In these processes, the thickness of deposited films can vary from one molecular layer to thousands, depending on specific applications or end-use requirements that can vary from simple protective coatings to functional films as, for instance, patterned films of π-conjugated polymers for electronic applications [122, 123]. One of these processes is spin coating, which is a simple and effective method to deposit thin and ultrathin homogenous films across planar substrates. Compared with other film forming processes, spin coating is perhaps the

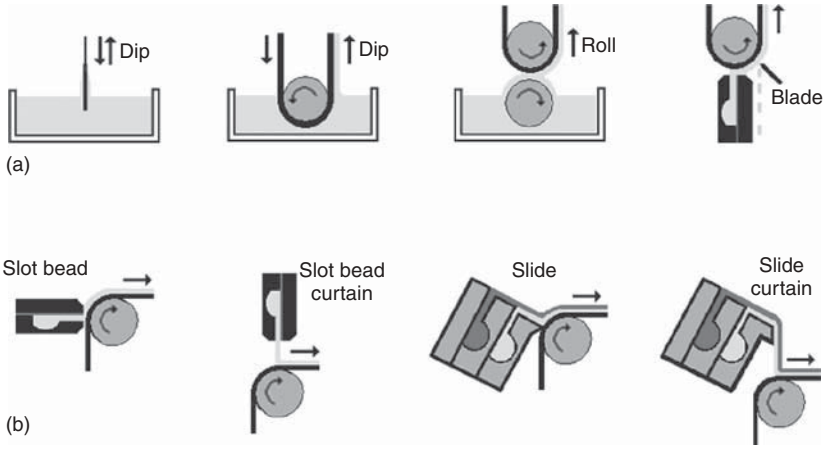

Figure 25.11 Schematic representation of (a) self-metered and (b) premetered coating processes.

simplest method to deposit thin films over a substrate, although small changes in the process parameters can greatly affect the final film characteristics and properties. Other techniques, including LB deposition, layer-by-layer (LbL) deposition, spraying, and epitaxy can be used for the deposition (from solution) of films as thin as one single molecular layer [118, 124–126].

25.4.1.3 Spin Coating Spin coating is a procedure which involves the deposition of uniform thin coating—typically having a thickness in the micron (thin) and submicron (thin > 200 nm > ultrathin) ranges and a total thickness variation of few nanometers—over a rotating flat substrate (or wafer) [127, 128]. In a few words, it is accomplished by flooding the substrate with a solution and rotating it at a constant speed (1000–8000 rpm) [117]. Curved, patterned, and many other specific surfaces can also be covered by this process [129–131]. Fluids of different nature, including sol–gel colloidal suspensions [132], polymer solutions [133], and hybrid materials [134], can also be processed by spin coating following similar procedures. The spin coating method is extensively used in microelectronics and related areas for the deposition of photoresists [135, 136], protective coatings [137], active layers in light emitting diodes [123], among others. This is also a common choice of method for research on thin and ultrathin functional films mainly due to the high quality of deposited films along with additional benefits when combined with various external fields [130].

The basic stages of the spin coating process are as follows:

1. Deposition of an excess volume of a solution onto the center of a substrate that might be held in a perfect horizontal position, either immobile (static dispense) or rotating at a relatively low speed (dynamic dispense). Other modes of deposition can be implemented [138].
2. Acceleration of the rotational speed of the substrate (spin-up).
3. Rotation of the substrate at a rotational speed that typically falls in the 10^3-10^4 rpm range (spin-off).
4. Evaporation of volatile components while the substrate is still rotating.

In standard practice, stages 1 and 2 take a minor fraction of time compared to that consumed in stages 3 and 4. A schematic representation of the spin coating stages is depicted in Figure 25.12.

As established long time ago, the film thinning arises basically from two distinct and quasi-simultaneous effects: spreading of the fluid caused by radial forces and evaporation of the solvent [128]. The spin coating process is not sensitive to the deposited volume as long as this suffices to cover the substrate; excess volume is ejected off the edge of the substrate [127, 139]. Most part of the solvent is evaporated during spinning at a rate that depends basically on the volatility of the solvent, the rotation rate, and the ambient conditions at the immediate film surroundings [114]. A postprocess drying treatment helps to eliminate the remaining volatile components and allows the film to equilibrate [140, 141]. In some cases the surrounding air phase is saturated with solvent vapor during film formation providing in this way sufficient time for chain mobility. This strategy has been used for instance for the recognition of the topology of prepatterned substrates and for fully developing a phase-separated microstructure in block copolymers in the film [130]. It has been also used to prevent film defects resulting from a rapid drying of highly volatile solvents [136]. The thickness and quality of the final free-solvent film (dry film) depends on multiple factors associated with the spin coating process, the solution and substrate characteristics, and the ambient conditions [117, 142]. In general, the higher the angular speed of spinning and the lower the concentration of the solution,

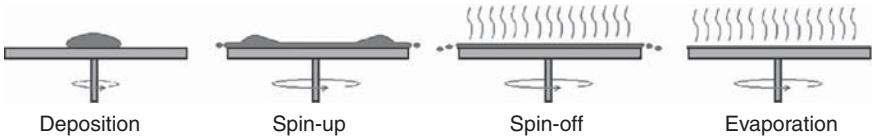

Figure 25.12 Basic stages in the spin coating process.

the thinner the film [123, 127, 128, 143]. The solvent and polymer characteristics are also key parameters in determining the film thickness [123, 133]. It is to point out that a minor variation in one of these and some other parameters can result in important deviations from the desired film characteristics; therefore, the repeatability is one of the most important challenges of spin coating. Commercial spin coaters are currently available for extensive production and experimental research. Technical details of commercial spin coaters are fairly accessible in the web.

Theory Because of its wide usage, the spin coating process has been much investigated from both the experimental and the theoretical points of view. There exist extensive experimental data on the process that has permitted not only to set up the process conditions for many specific polymer/solvent systems, but it has also permitted to understand the correlation of involved parameters and, therefore, to improve the spin coating process to comply with specific applications and research needs [114]. On the other hand, the theoretical or mathematical modeling of the spin coating process has been especially challenging due to the intricate coupling between fluid rheology and solvent evaporation, both having strong effects on the film thinning process [123].

Pioneering works on the mathematical modeling were very simple models in which flow and evaporation were decoupled. In a first approach by Emslie et al. [129], the film thinning (dh/dt) of a viscous flow of density ρ, deposited onto a flat substrate that rotates at constant angular velocity ω, was exclusively analyzed from the rheological point of view. The problem was simplified assuming Newtonian behavior (η_0), regular initial film thickness (h_0), no significant gravitational effects, no significant Coriolis forces, among others. The resulting equation (in cylindrical polar coordinates r, θ, z) allows the calculation of the film thickness (h) after a time t, starting with a liquid having a uniform initial thickness h_0 (Eq. 25.40). These authors have also modeled the case of liquids having irregular initial surface contours, demonstrating that thick layer regions thin out much more rapidly than thin ones, meaning that deposited fluids having a nonuniform initial surface profile tend to homogenize with time, confirming the utility of the spin coating process for producing uniform films of desired thickness [138]. Although not suitable for actual physical flow situations presented by most spin-coated fluids, this mathematical model has captured the essentials of the flow characteristics of liquids deposited onto a spin coater, and for this reason it has been frequently taken as the starting point of the film thinning modeling driven by centrifugal forces.

$$h = \frac{h_0}{\left[1 + 4\left(\frac{\rho\omega^2}{3\eta_0}\right) h_0^2 t\right]^{1/2}} \tag{25.40}$$

The work of Emslie et al. [129] was later extended by Acrivos et al. [144] to the case of power law non-Newtonian fluids, typical of concentrated polymer solutions. Contrary to the behavior observed in centrifuged Newtonian fluids, the non-Newtonian ones showed no tendency to form uniform films, even those having a uniform initial surface profile. The authors have thus concluded that spin-coated films of Newtonian fluids have a much better chance to be uniform. This is usually the case for sufficiently low concentrated polymer solutions.

In the second approach, Meyerhofer [128] introduced the film thinning (dh/dt)–evaporation rate (e) dependence to the Emslie, Bonner, and Peck model. In contrast to Equation 25.40, where h tends to vanish with time, Equation 25.41 predicts the formation of a solid film, which attains a finite final thickness (h_f) at time t_f. In this case, the hydrodynamic analysis should consider the viscosity–concentration dependence, but the problem has been simplified considering two separated subprocesses that omit such dependence, assuming that in the first stage the outflow dominates (concentration changes are neglected), but, once a specific thickness is attained, the flow stops and from this point on the second stage starts where the film thins only by evaporation. The mathematical expression for calculating the resulting final thickness for this model is as follows:

$$h_f = \frac{S_0}{L_0}\left(\frac{3\eta e}{2\rho_0\omega^2}\right)^{1/3} \tag{25.41}$$

where S_0 and L_0 are the initial volumes of the solute and solvent, respectively, $C_0 = S_0/(S_0 + L_0)$ and η is a power law function of concentration ($\eta = \eta_{solvent} + \eta_{solute}\, C^{\gamma}$). From this equation, it is clear that the film thickness is greatly influenced by the evaporation rate, as confirmed by Chen in an investigation on the solvent–evaporation effect on the spin coating of thin films of poly(vinyl butyryl) and cellulose acetate [114].

Bornside et al. [138] have developed a model for spin coating in which evaporation has been analyzed in terms of the mass flux (or mass transfer) from the liquid phase into the adjacent gas phase. Such a mass flux is controlled by a convection–diffusion process that depends on the solution concentration that increases as the solvent leaves the liquid phase. The characteristics of the gas phase in the close vicinity may also have a specific effect on the evaporation process. A modified model based on the equations of Meyerhofer and Bornside was used by Chang et al. [123] to predict the film thickness of spin-coated polymers. In their model, two equations were used: one to predict the wet film thickness, h_w, after spin coating but before drying and another to determine the final film thickness (h_f). The film thicknesses that they have theoretically predicted agree well with those experimentally determined, especially in solutions of low polymer concentration.

More recently, it was proposed that the flow dominates only for a short period before the "onset" of a relatively long intermediate flow/evaporation stage that culminates at high concentration when evaporation becomes dominant. The time interval for each one of these three stages was calculated by Cregan and O'Brien using a formal asymptotic approach [139]. These authors demonstrated that in the first stage (from t_0 to t') the flow dominates while the layer thickness decreases rapidly, then, in the second stage (from t' to t''), the flow and evaporation are equally important from an asymptotic point of view, and in the third stage the flow practically stops and the evaporation dominates letting the film to thin linearly. Figure 25.13 shows a schematic representation of different models of film thinning in a spin coating process.

Solution Thermodynamics in Spin Coating. A polymer solution confined between two surfaces (thin film) may show substantial differences in thermodynamic properties when compared to those in bulk [145]; this is because surface effects (important in thin films) may influence the phase equilibrium as well as the kinetics of demixing. Surface effects are important because they may lead to a specific lateral-phase segregation, to a surface-oriented phase separation, to the formation of a wetting layer or to the breakup of a surface layer, among others [146, 147].

The preparation of polymer films from spin coating involves rapid evaporation of the solvent along with the formation of segregated domains that grow until their size reaches the thickness of the film. Further growth of segregated domains is then limited by the geometrical constrains imposed by the film that thins continuously during the spin coating process. The lateral growth of segregated domains is determined by the complex interplay between different time-dependent processes such as elongational flow under a shear field, chain mobility, and solvent diffusion; therefore, the resulting morphology may be far from thermodynamic equilibrium. In this concern, Walheim et al. [141] studied polystyrene (PS)/solvent/poly(methyl methacrylate) (PMMA) solutions, which are interesting systems because PS and PMMA are strongly incompatible, show substantial differences in solubility in common solvents, and interact differently with substrates of different polarity. In addition, one of the two phases can be easily removed by using a selective solvent to obtain information from inside the film. These authors have reported microscopic images of thin films prepared from PS/solvent/PMMA solutions that exhibit a lateral-phase-separated morphology consisting of islands (PS or PMMA) whose composition differs from that of the surrounding continuous phase (PMMA or PS). They also examined the role of the substrate by using substrates of different surface energy. In substrates of high surface energy (polar) the PMMA forms a homogeneous layer and on top of this layer a phase-segregated domain structure is formed. A different polymer distribution may occur when the solution is deposited onto a substrate of low surface energy (nonpolar). In this hydrophobic surface the bottom layer consists mainly of PS rather than PMMA. The formation of a wetting PMMA (or PS) layer indicates the occurrence of a surface-oriented segregation process [148]. Segregation in thin films of PMMA–PS diblock copolymers has also been studied, showing some structural similarities driven by surface effects [149].

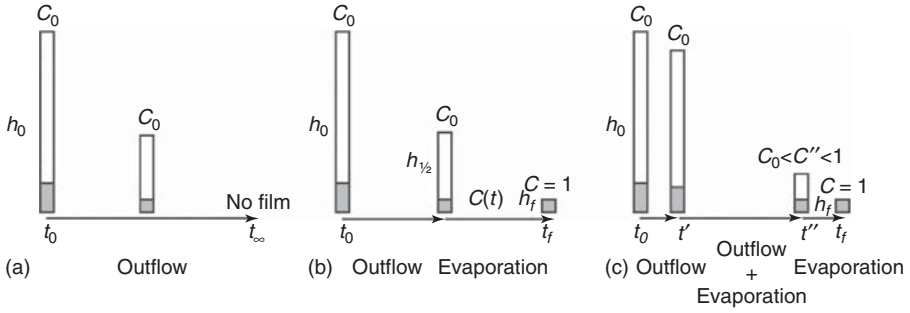

Figure 25.13 Graphical representation of (a) Emslie, Bonner and Peck, (b) Meyerhofer, and (c) Cregan and O'Brien models for the spin coating process.

25.4.1.4 Langmuir–Blodgett Deposition In the LB film deposition technique, a one-molecule-thickness (monolayer) film formed at an air–liquid interface is transferred onto a substrate [150]. The monolayer film (also known as *Langmuir film*) is built up with molecules partially ejected from the liquid (usually water) subphase as a result of polar/nonpolar interactions. This gas-like phase is then slowly compressed up to the formation of a floating two-dimensional solid film that may have the molecules laterally packed and with their polar head pointing toward the water side. This process is normally monitored through a surface pressure versus molecular area plot (or isotherm), which shows the transitions occurring from the less compressed gas-like phase to the solid phase, where molecules are closely packed [151]. Defects such as holes, collapsed regions, and grains can occur but they are, in general, reduced by taking extreme care during film preparation [152]. The monolayer films can be transferred onto hydrophilic or hydrophobic substrates. Most reported works on LB film deposition have been conducted with fatty-acid-type materials (soaps), for which a wealth of information on experimental data exist; however, the preparation of thin films with polymeric materials is of increasing interest, particularly for polymers showing appropriate amphiphilic properties to form monolayer and multilayer films [152, 153].

25.4.1.5 Layer-by-Layer Deposition The LbL deposition is performed by using alternating oppositely charged materials dissolved in an appropriate solvent [154, 155]. Other functionalities, such as hydrogen bonding, can also be used as the driving force for film assembly [156]. Different methods including dip coating, spin coating, and spray coating can be used for LbL deposition of thin films, although dip coating is the most preferred method [157]. One of the main advantages of the LbL deposition method is the high degree of control over the film thickness, which increases linearly as the number of deposited layers increases [155].

25.4.1.6 Epitaxy Epitaxial crystallization is a method of deposition of thin solid films from a solution. In this process a substance crystallizes (guest crystal) on the surface of a crystalline substrate (host crystal) of similar or different nature [126]. Examples of epitaxial crystallization range from single atom arrangements up to the deposition of complex synthetic and biological high molecular weight molecules [158]. In fact, many investigations have been devoted to the epitaxial crystallization of polymers to obtain thin crystalline films, particularly from a dilute polymer solution. Under this regime and favorable conditions, single polymer molecules are trapped on the substrate surface following a segmental contact that nucleates the formation of crystal overgrowths. The resulting molecular order of such overgrowths depends on different parameters including temperature, solution concentration, polymer characteristics (molecular weight, molecular architecture, etc.), solvent nature, and substrate type. Epitaxy can induce molecular arrangements that are not observed under ordinary crystallization conditions. A number of techniques of polymer film preparation by epitaxy on selected substrates have been employed [158–161]. One of the simplest techniques involves the preparation, at high temperature, of a dilute polymer solution using a high melting temperature substance that will act as a diluent and as a substrate [159, 161]. On cooling, the diluent crystallizes, providing surface substrates for the subsequent crystallization of the polymer. The substrate is then dissolved in an appropriate solvent and the remaining crystalline polymer is recuperated. Other simple method is the isothermal immersion method in which a substrate is first introduced into a slowly boiling polymer solution [162]. Then, this system is rapidly transferred to a thermostated bath heated at a desired crystallization temperature to induce the epitaxial growth. Next, the crystallization is stopped by dilution using the same solvent previously heated at the crystallization temperature. Finally, the substrate is dissolved at room temperature using a suitable solvent and the crystallized polymer is recuperated. Inorganic salts such as the NaCl-like alkali halides single crystals have been frequently used as templates [163], although organic substrates also induce well-developed epitaxial crystallization [126]. Polymer substrates have been successfully used as templates as well [126, 164]. Numerous examples of epitaxial crystallization from a polymer solution are reported in the literature [165, 166].

25.4.2 Fiber Forming Processes from Solution

Polymer fibers are normally manufactured through spinning processes in which a viscous liquid (melt or solution) is forced through multiple tiny holes (spinneret) to emerge as continuous filaments. The principal spinning processes from polymer solutions are wet, dry, and gel spinning. All three methods involve the formation of continuous filament strands by forcing the material through dies of specific geometry and the subsequent removal of the solvent to form solid filaments. A completely different method, the electrospinning process, has been developed to obtain nanoscale diameter filaments from polymer solutions.

25.4.2.1 Wet Spinning Wet spinning is a process in which a polymer solution is forced through a spinneret submerged in a coagulation bath (or wet bath), allowing the filaments to precipitate (solidify) as soon as they come out of the spinneret holes [167, 168]. These filaments are removed from the bath by a rotating roll and then collected in bundles, which are concurrently washed in successive extraction baths to eliminate residual solvent, and finally

dried. The solvent is selected according to the particular fiber to be spun, and the nonsolvent (coagulant), which is normally chemically inert to the film forming material, is selected according to both the film forming material and the extrusion solvent [169]. The as-spun fibers are drawn under specific conditions to obtain final dimensions. The morphology and final properties of filaments are highly dependent on coagulation [40, 170–172] and also on the drawing process that induces molecular orientation [173]. Acrylic [172], cellulose [40], aramid [174], spandex [175], among others [168], can be produced by this process.

25.4.2.2 Dry Spinning In this process a polymer solution is pumped through a spinneret and the emerging filaments are dried (solvent evaporation) by using a high temperature inert gas flow [176]. Solidified filaments are grouped into bundles before being collected on a take-up wheel. Dry spun fibers are normally drawn (stretched) either during or subsequent to spinning to effect orientation of polymer chains, increasing in this way the tensile strength of the material and other properties [177, 178]. Owing to environmental and safety reasons the use of this process is limited. This process may be used for the production of fibers of polymers such as acetate [179], acrylic [180], polyamides [177], polybenzimidazole (PBI) [181], and spandex [182]

25.4.2.3 Gel Spinning This is a process in which a gel is spun into fibers and then ultradrawn to reach final dimensions and strength [183, 184] This process is also known as dry–wet spinning because the fibers are first air dried, then cooled in a liquid bath. The gel is a semidilute solution with partially crystallized chains (liquid crystalline state) showing entanglement of low density that allows the polymer molecules to reach high orientation in the drawing process. The high orientation of molecules gives rise to the formation of high performance fibers normally showing an outstanding tensile strength property. Some high-strength polyethylene and aramid fibers are produced by gel spinning [183, 185].

25.4.2.4 Electrospinning Electrospinning is a method for the production of nanofibers. Although molten polymers have been successfully electrospun [186], electrospinning is above all a process for polymer solutions. In this process high voltage is applied to a polymer solution to create an electrically charged jet, which is continuously ejected from the tip of a capillary tube by the effect of an applied electric field [187]. Before reaching a collector, the jet loses the solvent by evaporation and the polymer molecules come close to each other to form nanoscale diameter fibers. The applied voltage induces electrical charges on the surface of the fluid (at the tip), which initially elongates up to the formation of a Taylor cone, and once the induced repulsive electrostatic force surpasses the surface tension of the fluid, an electrically charged jet is suddenly ejected toward an oppositely charged screen. This primary charged jet may split into multiple jets of different diameter.

Solution characteristics such as concentration, elasticity, viscosity, surface tension, nature of the solvent (or solvents), and conductivity, along with processing variables such as applied voltage, capillary tip to collector distance, and processing temperature, are important parameters in electrospinning [187]. All these characteristics may be considered to get free-defect continuous nanofibers of determined average diameter. In general, the fiber diameter is proportional to concentration and viscosity. As the viscosity of solutions is significantly reduced by heating, high concentrated solutions can be electrospun at high temperatures.

Electrospinning has been conducted with a variety of polymer solutions in different solvents at concentrations ranging from 0.5 to 30 wt%, although most reports indicate concentrations ranging from 10 to 20 wt%. Electrospinning is applicable to a wide range of polymers such as polyamides, polyester, and PBI [188], as well as to polymers such as DNA [189], polypeptides [190], or others like π-conjugated (or conducting) polymers [191].

REFERENCES

1. Parrish CF. Solvent, industrial. In: Grayson M, Eckroth D, editors. *Kirk-Othmer Encyclopedia of Chemical Technology*. 3rd ed. Volume 21. New York: John Wiley & Sons; 1983. p 377.
2. Fleischer D. Physical constants of the most common solvents. In: Brandrup J, Immergut EH, editors. *Polymer Handbook*. 3rd ed. New York: Wiley-Interscience Pub.; 1989. p III/29.
3. Rubin II. Injection molding of thermoplastics. In: Berins ML, editor. *SPI Plastics Engineering Handbook*. 5th ed. Boston: Kluwer Academic Publishers; 1991. p 133.
4. Wang JS, Porter RS. Rheol Acta 1995;34:496.
5. Berry GC, Fox TG. Adv Polym Sci 1968;5:261.
6. Patterson GB. *Physical Chemistry of Macromolecules*. 1st ed. New York: CRC Press, Taylor & Francis Group; 2007. p 43.
7. Erman B, Flory JP. Macromolecules 1982;15:806.
8. Daoud M, Bouchaud E, Jannik G. Macromolecules 1986;1955:19.
9. McKenna GB, Flynn KM, Chen Y. Polymer 1990;1937:31.
10. Yamauchi A. Gels: Introduction. In: Osada Y, Kijiwara K, editors. Gels Handbook, 1. Fundamentals. 1st ed. San Diego: Academic Press; 2001. p 4.
11. Russ T, Brenn R, Geoghegan M. Macromolecules 2003;36:127.
12. Sebille B. Solubilité des Polymères. In: Champetier G, editor. *Chimie Macromoléculaire II*. Paris: Hermann; 1972. p 65.

13. Blanks RF. Polym Plast Technol Eng 1977;8:13.
14. Kurata M. *Thermodynamis of Polymer Solutions*. MMI Press Polymer Monograph Series. 1st ed. New York: Harwood Academic Publishers; 1982. p 3.
15. De Gennes PG. *Scaling Concepts in Polymer Physics*. 1st ed. New York: Cornell University Press; 1979. p 19, 69.
16. Heil JF, Prausnitz JM. AICHE J 1966;12:678.
17. Candau F, Strazielle C, Benoit H. Eur Polym J 1976;12:95.
18. Hsu JP, Lin SH. Polymer 2003;44:8201.
19. Miller-Chou BA, Koenig JL. Prog Polym Sci 2003;28:1223.
20. Bercea M, Wolf BA. Macromol Chem Phys 2006;207:1661.
21. Krenz RA, Laursen T, Heidemann RA. Ind Eng Chem Res 2009;48:10664.
22. Graessley WW. Polymer 1980;21:258.
23. Daoud M, Cotton JP, Farnoux B, Jannink G, Sarma G, Benoit H, Duplessix R, Picot C, de Gennes PG. Macromolecules 1975;8:804.
24. Amirzadeh J, McDonnell ME. Macromolecules 1982;15:927.
25. Ying Q, Chu B. Macromolecules 1987;20:362.
26. Teraoka I. *Polymer Solutions: An Introduction to Physical Properties*. 1st ed. New York: John Wiley & Sons Inc.; 2002. p 63, 277.
27. Flory PJ, Krigbaum WR. J Chem Phys 1950;18:1086.
28. Barth HG, Mays JW. *Modern Methods of Polymer Characterization*. 1st ed. New York: John Wiley and Sons Inc.; 1991. p 201.
29. Nakamura Y, Akasaka K, Katayama K, Norisuye T, Teramoto A. Macromolecules 1992;25:1134.
30. Pfefferkorn P, Beister J, Hild A, Thielking H, Kulicke WM. Cellulose 2003;10:27.
31. Yu Y, DesLauriers PJ, Rohlfing DC. Polymer 2005;46:5165.
32. Sun T, Brant P, Chance RR, Graessley WW. Macromolecules 2001;34:6812.
33. Sanchez IC, Lacombe RH. Macromolecules 1978;11:1145.
34. Castells RC, Romero LM, Nardillo AM. Macromolecules 1996;29:4278.
35. Karimi M, Albrecht W, Heuchel M, Weigel T, Lendlein A. Polymer 2008;49:2587.
36. Kelley FN, Bueche F. J Polym Sci 1961;50:549.
37. Chatterjee AP, Schweizer KS. Macromolecules 1998;31:2353.
38. Chen X, Burger C, Wan F, Zhang J, Rong L, Hsiao BS, Chu B, Cai J, Zhang L. Biomacromolecules 2007;1918:8.
39. Lambourne R, Strivens TA. *Paint and Surface Coatings. Theory and Practice*. 2nd ed. Cambridge: Woodhead Publishing Ltd; 1999. p 1, 169.
40. Ruan D, Zhang L, Zhou J, Jin H, Chen H. Macromol Biosci 2004;4:1105.
41. Romdhane IH, Price PE, Miller CA, Benson PT, Wang S. Ind Eng Chem Res 2001;40:3065.
42. Flory PJ. J Chem Phys 1942;10:51.
43. Huggins ML. Ann New York Acad Sci 1942;43:1.
44. Kamide K, Dobashi T. Physical Chemistry of Polymer Solutions*:* Theoretical Background. 1st ed. Amsterdam: Elsevier Science B.V; 2000. p 1.
45. Sun SF. *Physical Chemistry of Macromolecules: Basic Principles and Issues*. 2nd ed. New Jersey: John Wiley & Sons Inc.; 2004. p 67, 96.
46. Pitzer KS, Brewer L. *Thermodynamics*. 2nd ed. New York: McGraw-Hill Inc; 1961. p 75.
47. Munk P. *Introduction to Macromolecular Science*. 1st ed. New York: John Wiley & Sons; 1989. p 217.
48. Flory PJ. *Principles of Polymer Chemistry*. 1st ed. Ithaca (NY): Cornell University Press; 1953. p 399, 495.
49. Flory PJ. *Statistical Mechanics of Chain Molecules*. New York: Hanser Publishers; 1989. p 1, 30.
50. Mattice WL, Suter UW. *Conformational Theory of Large Molecules: The Rotational Isomeric State Model in Macromolecular Systems*. 1st ed. New York: John Wiley & Sons Inc.; 1994. p 5.
51. de Gennes PG. Phys Lett 1972;A 38:339.
52. Edwards SF. Proc Phys Soc 1965;85:613.
53. Duxbury PM, de Queiroz SLA, Stinchcombe RB. J Phys Math Gen 1984;17:2113.
54. des Cloizeaux J, Noda I. Macromolecules 1982;15:1505.
55. Ottinger HC. Macromolecules 1985;18:1348.
56. Fisher ME, Sykes MF. Phys Rev 1959;114:45.
57. Hashizume J, Teramoto A, Fujita H. J Polym Sci Polym Phys Ed 1981;19:1405.
58. Huggins ML. J Am Chem Soc 1964;86:3535.
59. Patterson D. Rubber Chem Technol 1967;40:1.
60. Li J, Wan Y, Xu Z, Mays JW. Macromolecules 1995;28:5347.
61. Duval M, Coles HJ. Rev Phys Appl 1980;15:1399.
62. Fujita H, Norisuye T. Macromolecules 1985;18:1637.
63. Mitchell J Jr,. *Applied Polymer Analysis and Characterization*. Volume II. Munich: Hanser; 1992. p 3.
64. Wilson GM. J Am Chem Soc 1964;86:127.
65. Renuncio JAR, Prausnitz JM. Macromolecules 1976;9:898.
66. Rubio RG, Renuncio JAR. Macromolecules 1980;13:1508.
67. Sanchez IC, Lacombe RH. J Phys Chem 1976;80:2352.
68. Lacombe RH, Sanchez IC. J Phys Chem 1976;80:2568.
69. Panayiotou C, Vera JH. Polym J 1982;14:681.
70. Danner RP, High MS. Fundamentals of polymer solution thermodynamics. In: Danner RP, High MS, editors. *Handbook of Polymer Solution Thermodynamics*. 1st ed. New York: Design Institute for Physical Property Data AIChE; 1993. p 3.
71. Kumar SK, Suter UW, Reid RC. Ind Eng Chem Res 1987;26:2532.
72. Mansouri GA. Condens Mater Phys 2005;8:389.
73. Blanks RF, Prausnitz JM. Ind Eng Chem Fundamentals 1964;3:1.
74. Orwoll RA. Solubility of polymers. In: Kroschwitz JI, editor. *Concise Encyclopedia of Polymer Science and*

Engineering. 1st ed. New York: John Wiley & Sons; 1990. p 1066.

75. Hansen CM. The three dimensional solubility parameter and solvent diffusion coefficient. Their importance in surface coating formulation [PhD thesis]. Technical University of Denmark Copenhagen; 1967.
76. Belmares M, Blanco M, Goddard WA, Ross RB, Caldwell G, Chou S-H, Pham J, Olofson PM, Thomas C. J Comput Chem 2004;1814:25.
77. Chanda M, Roy SK. *Plastics Technology Handbook*. 2nd ed. New York: Marcel Dekker Inc.; 1993. p 40.
78. Schultz AR, Flory PJ. J Am Chem Soc 1952;74:4760.
79. Utracki LA. *Polymer Alloys and Blends: Thermodynamics and Rheology*. 1st ed. New York: Hanser Publishers; 1990. p 29.
80. Rauwendaal C. *Polymer Mixing: A Self Study Guide*. 1st ed. Munich: Hanser; 1998. p 25.
81. Van der Haegen R, Kleintjens LA. Pure Appl Chem 1989;61:159.
82. Saeki S, Kuwahara N, Konno S, Kaneko M. Macromolecules 1973;6:246.
83. Schouterden P, Groeninckx G, Van der Heijden B, Jansen F. Polymer 1987;2099:28.
84. Okamoto H, Sekikawa K. J Polym Sci 1961;55:597.
85. Favre E, Nguyen QT, Clement R, Neel J. Eur Polym J 1996;32:303.
86. Sariban A, Binder K. Macromolecules 1988;21:711.
87. Lutz JT Jr,. *Thermoplastic Polymer Additives: Theory and Practice*. 1st ed. New York: Marcel Dekker Inc.; 1989. p 1.
88. Sabadini E, Assano EM, Atvars TDZ. J Appl Polym Sci 1997;65:595.
89. Moses CL, Robelo LPN, Van Hook WA. J Polym Sci B Polym Phys 2003;41:3064.
90. Striolo A, Prausnitz JM, Bertucco A, Kee RA, Gauthier M. Polymer 2001;42:2579.
91. Wachter AH, Simon W. Anal Chem 1969;41:90.
92. Meeks AC, Goldfarb IJ. Anal Chem 1967;39:908.
93. Berry GC. J Phys Chem 1966;70:1194.
94. Law PW, Longdon A, Willins GG. Macromol Symp 2004;208:293.
95. Reinehr U, Herbertz T. inventors; Bayer Aktiengiesellschaft. US patent 4,650,624. 1987.
96. Siemann U. Progr Colloid Polym Sci 2005;130:1.
97. Schruben DL, Gonzalez P. Polym Eng Sci 2000;40:139.
98. Tang ZG, Black RA, Curran JM, Hunt JA, Rhodes NP, Williams DF. Biomaterials 2004;25:4741.
99. Tsujimoto T, inventors; Fujifilm Corporation. US patent 7,390,434. 2008.
100. Tsujimoto T, inventors; Fujifilm Corporation. US patent 7,361,295 B2. 2008.
101. Abiru D, inventors; Fujifilm Corporation. US patent 7,891,861 B2. 2011.
102. Li Z, Jiang C. J Appl Polym Sci 2001;82:283.
103. Schruben DL, Kumble D. Polym Eng Sci 1996;36:2494.
104. Kunst B, Sourirajan S. J Appl Polym Sci 1983;1970:14.
105. Hansen CM. *Ind*. Eng Chem Prod Res Dev 1970;9:282.
106. Bierwagen GP. Corrosion and its control by coatings. In: Bierwagen GP, editor. *Organic Coatings for Corrosion Control*. ACS Symposium Series. 1st ed. Volume 689. Washington (DC): Oxford University Press; 1998. p 1.
107. Wicks ZW Jr,, Jones FN, Pappas SP. *Organic Coatings Science and Technology*. 2nd ed. New York: Wiley-Interscience; 1999. p 1.
108. Smith RL. Environ Health Perspect 1984;57:1.
109. Athawale VD, Nimbalkar RV. J Am Oil Chem Soc 2011;88:159.
110. Bourtoom T. Int Food Res J 2008;15:237.
111. Isono Y, Nagasawa M. Macromolecules 1980;13:862.
112. Moore JE, inventors; General Electric Company. US patent 4,902,725. 1990.
113. Bongiovanni R, Montefusco F, Priola A, Macchioni N, Lazzeri S, Sozzi L, Ameduri B. Progr Org Coating 2002;45:359.
114. Chen BT. Polym Eng Sci 1983;23:399.
115. Ton-That C, Shard AG, Bradley RH. Langmuir 2000;16:2281.
116. Cisneros-Zevallos L, Krochta JM. J Food Sci 2003;68:503.
117. Weill A, Dechenaux E. Polym Eng Sci 1988;28:945.
118. Krogman KC, Zacharia NS, Schroeder S, Hammond PT. Langmuir 2007;23:3137.
119. Jiang X, Hammond PT. Langmuir 2000;16:8501.
120. Ruschak KJ. Annu Rev Fluid Mech 1985;17:65.
121. Weinstein SJ, Ruschak KJ. Annu Rev Fluid Mech 2004;36:29.
122. Kobayashi A, Saiki Y, Watanabe K. Nanocapacitor: new tantalum capacitor with conducting polymer. In: Rupprecht L, editor. *Conductive Polymers and Plastics in Industrial Applications*. 1st ed. New York: Plastic Design Library; 1999. p 167.
123. Chang CC, Pai CL, Chen WC, Jenekhe SA. Thin Solid Films 2005;479:254.
124. Kolasinska M, Krastev R, Gutberlet T, Warszynski P. Langmuir 2009;25:1224.
125. Chen W, McCarthy TJ. Macromolecules 1997;30:78.
126. Wittmann JC, Lotz B. Prog Polym Sci 1990;15:909.
127. Hall DB, Underhill P, Torkelson JM. Polym Eng Sci 2039;1998:38.
128. Meyerhofer D. J Appl Phys 1978;49:3993.
129. Emslie AG, Bonner FT, Peck LG. J Appl Phys 1958;29:858.
130. Lee G, Sung Jo P, Yoon B, Hee Kim T, Acharya H, Ito H, Kim HC, Huh J, Park C. Macromolecules 2008;41:9290.
131. Kim S, Lee J, Jeon SM, Lee HH, Char K, Sohn BH. Macromolecules 2008;41:3401.
132. Britten JB, Thomas IM. J Appl Phys 1992;71:972.
133. Schubert DW, Dunkel T. Mat Res Innovat 2003;7:314.
134. Beek WJE, Wienk MM, Kemerink M, Yang X, Janssen RAJ. J Phys Chem B 2005;109:9505.

135. Chandrasekhar P. *Conducting Polymers: Fundamentals and Applications*. 1st ed. Boston: Kluwer Academic Publishers; 1999. p 591.
136. Gurer E, Litvak H, Savage R, inventors. US patent 6,027,760. 2000.
137. Washo BD. IBM J Res Dev 1977;21:190.
138. Bornside DE, Macosko CW, Scriven LE. J Imag Technol 1987;13:122.
139. Cregan V, O'Brien SBG. J Colloid Interface Sci 2007;314:324.
140. Frank B, Gast AP, Russell TP, Brown HR, Hawker C. Macromolecules 1996;29:6531.
141. Walheim S, Böltau M, Mlynek J, Krausch G, Steiner U. Macromolecules 1997;30:4995.
142. Gupta SA, Gupta RK. Ind Eng Chem Res 1998;37:2223.
143. Affrossman S, Henn G, O'Neill SA, Pethrick RA, Stamm M. Macromolecules 1996;29:5010.
144. Acrivos A, Shah MJ, Petersen EE. J Appl Phys 1960;51:963.
145. Reich S, Cohen Y. J Polym Sci Polym Phys Ed 1981;19:1255.
146. Geoghegan M, Jones RAL, Payne RS, Sakellariou P, Clough AS, Penfold J. Polymer 1994;2019:35.
147. Vaynzof Y, Kabra D, Zhao L, Chua LL, Steiner U, Friend RH. ACS Nano 2011;5:329.
148. Winesett DA, Ade H, Sokolov J, Rafailovich M, Zhu S. Polym Int 2000;49:458.
149. Mayes AM, Russel TP, Bassereau P, Baker SM, Smith GS. Macromolecules 1994;27:749.
150. Reitzel N, Greve DR, Kjaer K, Howes PB, Jayaraman M, Savoy S, McCullough RD, McDevitt JT, Bjørnholm T. J Am Chem Soc 2000;122:5788.
151. de Boer B, van Hutten PF, Ouali L, Grayer V, Hadziioannou G. Macromolecules 2002;35:6883.
152. Somanathan N, Pandiyarajan CK, Goedel WA, Chen WC. J Polym Sci B Polym Phys 2009;47:173.
153. Wijekoon WMKP, Wijaya SK, Bhawalkar JD, Prasad PN, Penner TL, Armstrong NJ, Ezenyilimba MC, Williams DJ. J Am Chem Soc 1996;118:4480.
154. Lee SH, Balasubramanian S, Kim DY, Viswanathan NK, Bian S, Kumar J, Tripathy SK. Macromolecules 2000;33:6534.
155. Smith RR, Smith AP, Stricker JT, Taylor BE, Durstock MF. Macromolecules 2006;39:6071.
156. Stockton WB, Rubner MF. Macromolecules 1997;30:2717.
157. Zucolotto V, He JA, Constantino CJL, Barbosa Neto NM, Rodrigues JJ Jr,, Mendoça CR, Zílio SC, Li L, Aroca RF, Oliveira ON Jr,, Kumar J. Polymer 2003;44:6129.
158. Sun LH, Xu CY, Yu F, Tao SX, Li J, Zhou H, Huang S, Tang L, Hu J, He JH. Cryst Growth Des 2010;10:2766.
159. Wittmann JC, Lotz B. J Polym Sci Polym Phys Ed 1981;19:1837.
160. Wittmann JC, Lotz B. J Polym Sci Polym Phys Ed 1981;19:1853.
161. Lotz B, Wittmann JC. J Polym Sci Polym Phys Ed 1986;24:1559.
162. Sano M, Sandberg MO, Yoshimura S. Langmuir 1994;10:3815.
163. Fujita M, Hamada N, Tosaka M, Tsuji M, Kohjiya S. J Macromol Sci Phys 1997;36:681.
164. Petermann J, Xu Y, Loos J, Yang D. Polymer 1992;33:1096.
165. Shen Y, Yang D, Feng Z. J Mater Sci 1991;26:1941.
166. Cartier L, Okihara T, Ikada Y, Tsuji H, Puiggali J, Lotz B. Polymer 2000;41:8909.
167. Watthanaphanit A, Supaphol P, Furuike T, Tokura S, Tamura H, Rujiravanit R. Biomacromolecules 2009;10:320.
168. Yan J, Zhou G, Knight DP, Shao Z, Chen X. Biomacromolecules 2010;11:1.
169. Hoxie HM, inventors; American Viscose Corporation. US patent 2,577,763. 1951.
170. Oh SC, Wang YS, Yeo YK. Ind Eng Chem Res 1996;35:4796.
171. Hirano S. Macromol Symp 2001;168:21.
172. Ji BH, Wang JH, Wang CG, Wang YX. J Appl Polym Sci 2008;108:328.
173. Um C, Ki CS, Kweon HY, Lee KG, Ihm DW, Park YH. Int J Biol Macromol 2004;34:107.
174. Jassal M, Ghosh S. Indian J Fibre Textil Res 2007;22:290.
175. Martin KE, Bing-Wo RD, Lock RL, inventors; In-Vista Technologies S.A.R.L. WO 2010/111088. 2010.
176. Gogolewski S, Pennings AJ, inventors; Medtronic Inc. US patent 4,915,893. 1990.
177. Gogolewski S, Pennings AJ. Polymer 1985;26:1394.
178. Smith P, Lemstra PJ, inventors; Stamicarbon B. V. US patent 4,344,908. 1982.
179. Brazinsky I, Williams AG, LaNieve HL. Polym Eng Sci 1975;15:834.
180. Reinehr U, Uhlemann H, inventors; Bayer Aktiengiesellschaft. US patent 4,457,884. 1984.
181. Tan M, inventors; Celanese Corporation. US patent 4,263,245. 1981.
182. Houser NE, Bakker W, Dreibelbis RL, inventors; E. I. Du Pont de Nemours and Company. US patent 5,362,432. 1994.
183. Barham PJ, Keller A. J Mater Sci 1985;20:2281.
184. Hoogsteen W, van der Hooft J, Postema AR, ten Brinke G, Pennings AJ. J Mater Sci 1988;23:3459.
185. Pennings AJ, van der Hooft RJ, Postema AR, Hoogsteen W, ten Brinke G. Polym Bull 1986;16:167.
186. Larrondo L, St John Manley R. J Polym Sci Polym Phys Ed 1981;19:909.
187. Huang ZM, Zhang YZ, Kotaki M, Ramakrishna S. Comp Sci Technol 2003;63:2223.
188. Kim JS, Reneker DH. Polym Eng Sci 1999;39:849.
189. Fang X, Reneker DH. J Macromol Sci Phys 1997;36:169.
190. Khadka DB, Cross MC, Haynie DT. Appl Mater Interfaces 2011;3:2994.
191. Srivastava Y, Marquez M, Thorsen T. J Appl Polym Sci 2007;106:3171.